Flame Spray Pyrolysis of Tin Oxide Based Pt Catalysts for PEM Fuel Cell Applications

SCHOLARONE™
Manuscripts

Flame spray pyrolysis of tin oxide-based Pt catalysts for PEM fuel cell applications

Paul I. Dahl[1,*], Luis C. Colmenares[1,2], Alejandro O. Barnett[1], Scott Lomas[1], Per E. Vullum[1], Jannicke H. Kvello[1], Julian R. Tolchard[1], Sidsel M. Hanetho[1], Tommy Mokkelbost[1]

[1] SINTEF Materials and Chemistry, NO-7465 Trondheim, Norway
[2] Current address: IK4-CIDETEC. Unit of Materials for Energy, 2014 San Sebastián, Spain

*Corresponding author: paul.inge.dahl@sintef.no

ABSTRACT

SnO_2 doped with Sb and Nb has been investigated for its use as catalyst support materials replacing carbon to enhance PEM fuel cells stability. Nanostructured powders of various doping levels were prepared by flame spray pyrolysis (FSP). The specific requirements of surface area >50 m^2g^{-1} and electronic conductivity >0.01 Scm^{-1} were obtained, and pore sizes ranging mainly from 10 to 100 nm. Pt particles (9-20 wt.% in loading targeted) of ~1 nm well dispersed in Sb-doped SnO_2 was prepared by a one-step FSP procedure providing microstructures of high interest for further investigations as cathode in PEM fuel cells.

INTRODUCTION

Nanostructured materials are gaining widespread use, requiring new approaches to powder synthesis with respect to increased production while maintaining proper safety procedures and requested material properties. Flame spray pyrolysis (FSP) is an excellent tool for pioneering development of complex nanomaterials for various applications and is also a scalable process already being investigated by commercial powder producers [1]. Such nanomaterials are of interest for electrodes in various energy applications such as PEM fuel cells (PEMFCs) where high conductivity, high surface area, well defined and sustainable pore structure/size distribution, stability and corrosion resistance are required material properties [2, 3].

In the present work FSP is applied to produce and investigate properties of tin-based oxide materials to be used as cathode catalyst support in PEMFCs, offering high electrochemical stability and corrosion resistance for this application as compared to carbon [4-6]. SnO_2-based materials synthesized by FSP are already reported in the literature for gas sensor applications [7-10], however, FSP is to our knowledge not applied for supported catalyst particles for PEMFCs. SnO_2 is a semiconductor, and in this work we elaborate on using antimony and niobium as dopants ($Sn_{1-x}M_xO_{2\pm\delta}$, x=0.00-0.15, M=Sb/Nb). Sb is introduced to enhance the electronic conductivity, required for the PEMFCs' support material, while Nb is added with the intention of supressing the segregation of Sb to the surface, as observed in contact with Pt-catalyst particles [11]. The synthesized support powders are compared with the same compositions prepared by co-precipitation (Co-P). Pt-catalyst is introduced to the SnO_2-based support through a direct one-step FSP synthesis and the results are compared against Pt deposited through well-established polyol-based and formic acid based deposition routes. In addition to the benefit of being a simple, one-step synthesis route, FSP also offers the production of supported catalyst particles using chlorine free precursors, eliminating potential poisoning issues in the fuel cell.

Within the ongoing European project SMARTCat, three physical properties are defined for the screening of suitable cathode catalyst support materials for PEMFCs;

1. A specific surface area (as measured by BET) of ≥ 50 m^{2}g^{-1}
2. Homogenous microstructure with a pore size distribution (PSD) of 20-150 nm
3. Electronic conductivity, $\sigma \geq 0.01$ Scm^{-1}

The prepared materials have been evaluated by physical characterization (XRD, BET, TEM) and with respect to electrical conductivity. Observed effects of Sb/Nb-doping are discussed and the morphology of the developed supports with Pt catalyst particles presented.

EXPERIMENTAL

Nanostructured tin-based oxide powders for use as cathode catalyst support materials in PEMFCs were synthesized by FSP using procedures similar to those reported in the literature [7, 8, 12]. Tin(II) 2-ethylhexanoate, antimony(III) ethoxide and niobium(V) ethoxide were used as precursors dissolved in p-xylene at a total cation concentration of ~0.40 M. For the one-step FSP synthesis of the same support materials with Pt included, platinum(II) acetylacetonate was dissolved in acetone and then added to the pre-made precursor solution of the Sn-based material. In this case, the total cation concentration of the support was reduced to ~0.20 M, in a 50:50 mixture (by volume) of p-xylene and acetone. The FSP was performed using a NPS10 apparatus (Tethis S.p.A.). The precursor/solvent mixtures were sprayed into a flame (CH$_4$/O$_2$ flow rates: 1.5/3.0 L/min) using a liquid flow rate of 5 mL/min and 5 L/min flow of dispersion gas (oxygen or nitrogen). A pressure drop (dispersion gas at nozzle tip) of ~2.0 bars was used and the powders were collected on a glass microfiber filter (Whatman GF6). The as-synthesized powders were ball milled for 18 hours in isopropanol using 5 mm YSZ balls in a rotating bottle with a subsequent drying and heat treatment at 550°C for 1 hour in ambient air.

While the focus of the present paper is the FSP powders, the comparing Co-P synthesis is briefly summarized. Tin(II) chloride, antimony(III) chloride and niobium(V) ethoxide was dissolved in isopropanol before addition of 2 M ammonium hydroxide. After overnight stirring repeated centrifugation and washing with isopropanol and water. The final powder was calcined at 550°C in ambient air for 2 hours. Deposition of Pt particles (20 wt.%) on synthetized SnO$_2$-based supports was done by polyol and formic acid methods. Polyol synthesis method has been employed for synthesis of powders and colloids of many different metals and is described elsewhere [13]. In the case of formic acid method, the Pt precursor is reduced by the acid in an aqueous solution at 80 °C [14]. In both cases the resulting samples is extensively washed with water to remove chlorine and subsequently dried at least at 120 °C for 12 hours.

The as-synthesized powders were analysed with respect to specific surface area and pore size distribution by N$_2$ adsorption/desorption measurements (BET) (Micromeritics Tristar). For TEM analysis, the prepared powders were dispersed in ethanol and a droplet was transferred to a holey carbon coated Cu TEM-grid. TEM was performed with a double Cs corrected, coldFEG JEM ARM200F, operated at 200 kV. X-ray diffraction (XRD) was performed using a Bruker D8 Focus diffractometer with Cu Kα radiation and LynxEye detector. The diffraction data was analysed using the Rietveld method as implemented in the TOPAS software by Bruker.

Two-probe measurements were performed on compressed (~56 bar) oxide powders to determine the electronic conductivities. Based on the measured height of the powder column between two pistons, the apparent conductivities of the samples were determined by applying (at a scan rate of 20mV/s) the following bias sequence: *1)* 100 cycles between -200 and 200 mV, *2)* 70 cycles between -400 and 400 mV, *3)* 100 cycles between -200 and 400 mV. This method resulted in a standard deviation of 10-15%. The apparent conductivity is reported as an average of the number of applied cycles.

RESULTS

Surface area of as-synthesized support materials without any catalyst particles is plotted as a function of antimony and niobium doping level in Figure 1, for both FSP and Co-P powders. It is evident that the surface area increases with the doping level for both dopants and synthesis procedures, however the effect is less severe for the powders prepared by FSP. Sb and Nb is reported to segregate to the surface as the dopant level increases and hence, inhibiting the particle growth. This phenomenon is known as "solute drag inhibiting growth" where one component segregates easier to grain boundary [15]. The higher BET surface area of FSP powder compared to Co-P ones is mainly associated to their microstructure (higher microporosity).
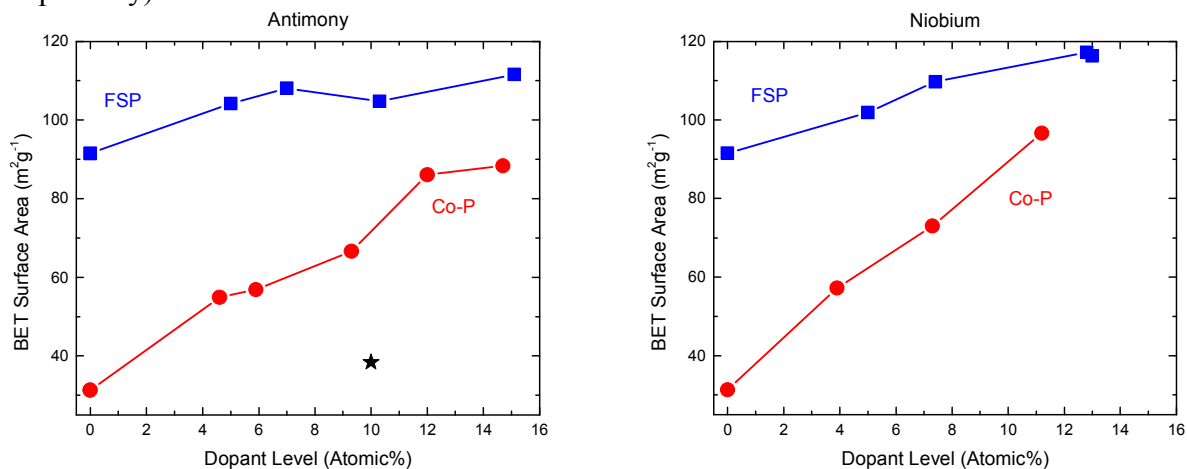

Figure 1. Surface area of as synthesized tin oxide powders prepared by FSP and Co-P as a function of Sb and Nb doping. Star in graph to the left indicate data from commercial material.

TEM images of as-synthesized and post treated (milling and heat treatment at 550°C) powders of $Sn_{0.95}Sb_{0.05}O_{2+\delta}$ are presented in Figure 2. A significant growth of the crystalline particles is observed (reducing the surface area to ~60 m^2g^{-1}), which is desired as it is expected to enhance the particles connectivity (electronic grain boundary effect) and hence also the electronic transport (conductivity) of the powders.
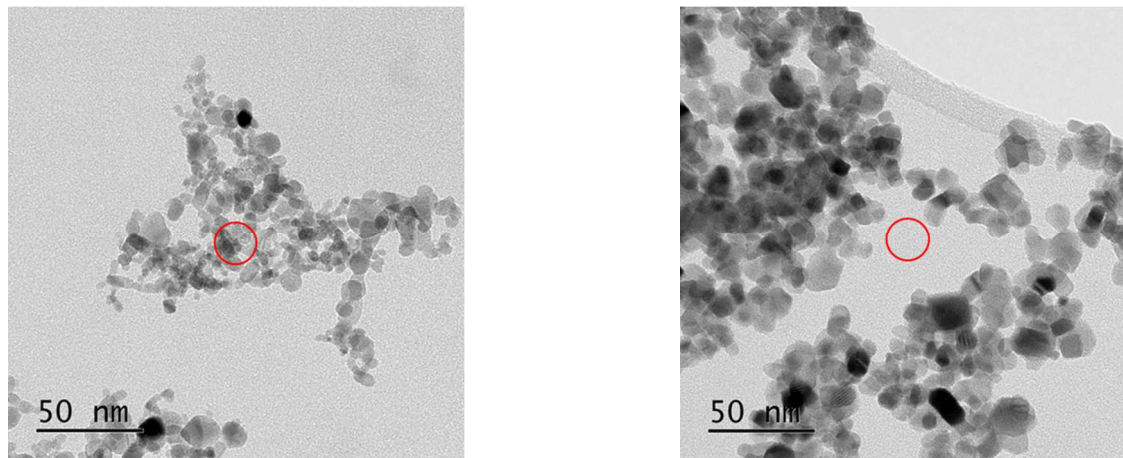

Figure 2. TEM images of as-synthesized $Sn_{0.95}Sb_{0.05}O_{2\pm\delta}$ (left), and post treated (milled and heat treated at 550°C, 1 hour) (right). The added rings are exactly 20 nm in diameter.

From nitrogen adsorption/desorption measurements the pores were found in the region required (20-150 nm) for the FSP powders, independent of doping level. This is due to the rapid FSP synthesis method having more effect over the microstructure than small variations in the chemical composition. For the Co-P powders the pore size distribution varied but did not follow any clear trend with doping level, e.g. it was found < 10 nm for 7.5% antimony doping.

The electronic conductivity of as-synthesized tin-based support powders is presented in Figure 3 a). The conductivity increases by more than 3 orders of magnitude up to a Sb-doping level of 7 atomic %. Beyond this Sb-doping level no significant increase is observed, in agreement with what is reported in the literature [11, 12]. Doping with 5-valent Nb does not enhance the conductivity. The cause of this lowering conductivity in niobium doped samples is assumed to be due to insulating layers (or separate phase as mentioned above) of Nb (Nb_xO_y) forming on the surface of particles, however is added together with Sb with the intention of suppressing the Sb segregation towards the interface between Pt catalyst and support material, as previously demonstrated [11]. As shown in Figure 3 b), the conductivity of the Sb doped FSP powders is significantly enhanced by the post-treatment in form of milling and heat treatment at 550°C, exceeding that of the commercial reference sample as well as the Co-P powders for doping levels < 10% Sb. The FSP powder with 5% Sb had a conductivity of 0.40 S/cm, comparable to 0.83 S/cm reported by Yin et al. for optimized 5% Sb doped powder, [16].
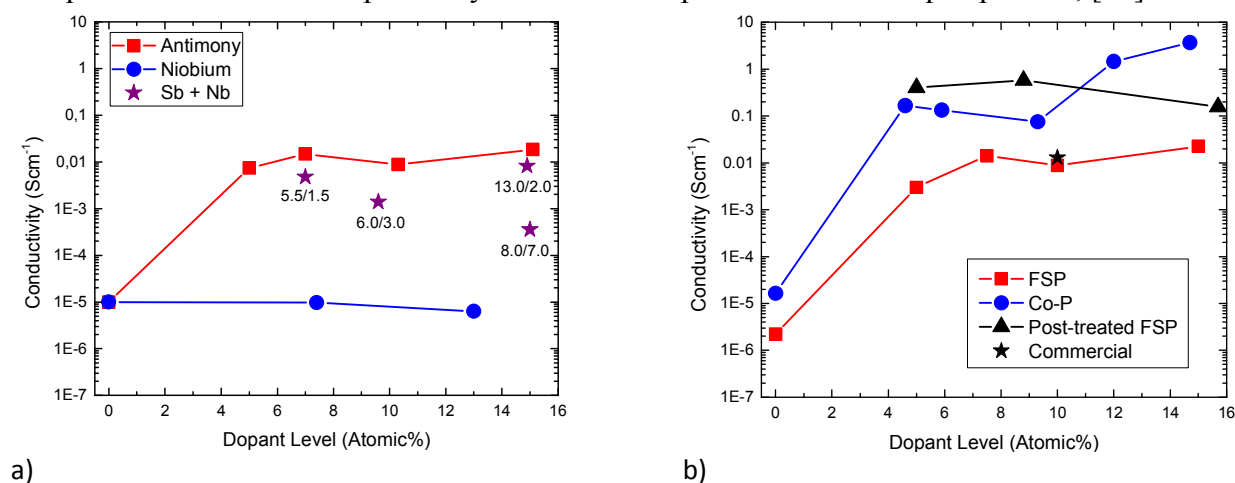

a)   b)

Figure 3. Electronic conductivity of as-synthesized Sn-based oxides prepared by FSP (a) and compared post-treated FSP powders, Co-P powders and commercial reference (b).

The XRD analysis of the one-step FSP synthesized powders with 9 and 20 wt.% Pt are shown in Figure 4. From these data, the average crystallite size of the $Sn_{0.935}Sb_{0.065}O_{2+\delta}$ support was calculated to ~5 nm, as compared to ~30 nm for the Pt catalyst crystallites.

Microstructures of Pt catalyst particles deposited on tin-based oxide support materials are depicted in Figure 5. The typical issues of large clusters of ~5 nm Pt particles obtained by polyol- and formic acid methods for depositing 20 wt.% Pt onto prepared $Sn_{0.95}Sb_{0.05}O_{2+\delta}$ powders are presented in Figure 5 a)

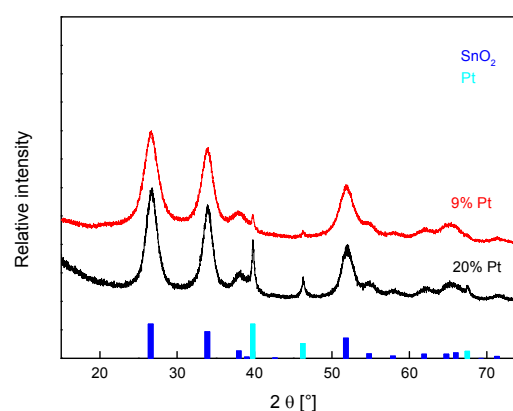**Figure 4.** XRD analysis of Pt supported on $Sn_{0.935}Sb_{0.065}O_{2+\delta}$ by one-step FSP route.

and b), respectively. In contrast, the one-step FSP procedure, as presented in Figure 5 c) and d), show nicely dispersed ~1 nm Pt particles on $Sn_{0.935}Sb_{0.065}O_{2+\delta}$ support particles. Whereas TEM analysis indicate that the ~1 nm Pt particles are crystalline, these are too small to be detected in XRD. However, the appearance of larger Pt particles of ~20 nm, as seen in Figure 5 c), explains the findings from XRD. XRD analysis indicate an increased amount of larger Pt particles with increased loading, indicating the support may be saturated with ~1 nm particles at a loading lower than 9 wt.% Pt. However, the larger particles may also be a result of un-optimized FSP conditions or precursor solution, e.g. resulting in formation of colloidal particles.
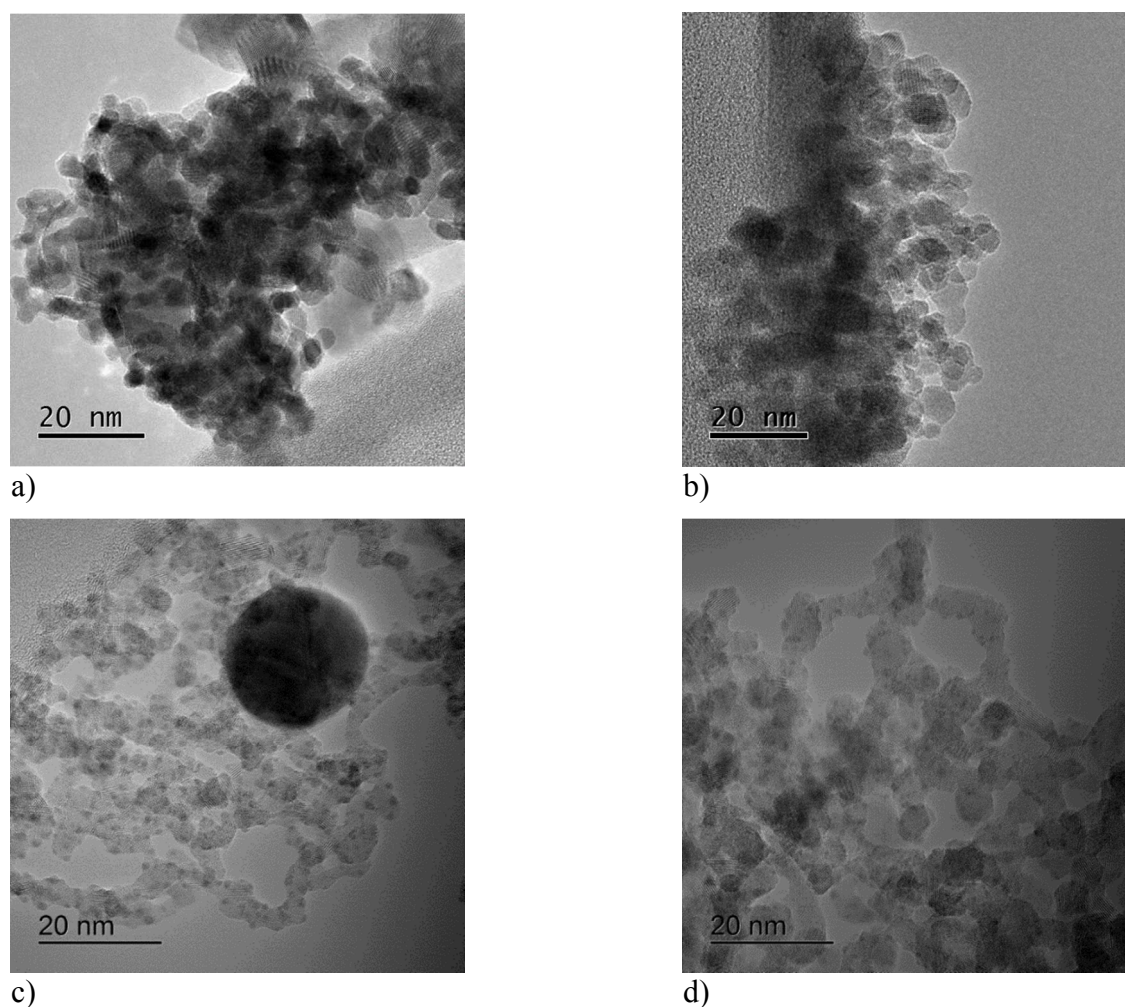

a)

b)

c)

d)

Figure 5. TEM images of large clusters of ~ 5 nm Pt particles on $Sn_{0.95}Sb_{0.05}O_{2\pm\delta}$ deposited by polyol- and formic acid methods, a) and b) respectively, and ~ 1 nm Pt particles dispersed on $Sn_{0.935}Sb_{0.065}O_{2\pm\delta}$ by one-step FSP procedure, before c) and after d) milling and heat treatment. All samples were prepared with the aim of 20 wt.% Pt loading.

The small Pt particles we found are comparable with results obtained by Teoh et al. for 0.1-4.0 wt.% Pt on TiO_2 by one-step FSP synthesis [17]. In our case the Pt loading is higher (9-20 wt.%), and despite the material system, precursor solutions and process conditions are different, it is worth remarking that the Pt particles are smaller (~1 nm) than those obtained on TiO_2 by Teoh et al. (1.4-2.5 nm). The size of the Pt particles was measured, providing a size distribution

as presented in Figure 6. The mean Pt particle size was reduced from 1.34 to 0.94 nm upon post treatment, possibly due to the removal of thin Pt oxide layers.

Figure 6. Pt particle size distribution from TEM analysis for the samples depicted in Figure 5 c) and d).

CONCLUSIONS

Nanostructured Sn-based oxide powders doped with Sb to optimize conductivity and co-doped with Nb in an attempt to suppress Sb segregation are prepared by flame spray pyrolysis. The microstructural properties of the synthesized powders are better suited as catalyst support materials for PEM fuel cells compared to those prepared by co-precipitation. The requirements for such supports are fulfilled, that is;

1) Surface area >50 m^2g^{-1}.
2) Electronic conductivity >0.01 Scm^{-1}.
3) Pore size distribution in the range of 20-150 nm.

These catalyst supports seem suitable for potential replacement of state-of-the-art carbon to improve stability and durability of the PEM fuel cells.

Additionally, 9-20 wt.% Pt particles of ~1 nm well dispersed in Sb-doped SnO_2 was prepared by a one-step FSP procedure. These microstructures seems superior in term of cleanness, Pt particle dispersion and reproducibility to those obtained by polyol- and formic acid methods for Pt deposition. The small Pt particle size could result in good catalytic performance with lower Pt loading, making this one-step synthesis interesting for cathode materials in PEM fuel cells.

ACKNOWLEDGMENTS

REFERENCES

1. W.Y. Teoh, R. Amal, and L. Mädler, Nanoscale, 2010. **2**(8): p. 1324-1347.
2. S. Sharma, and B.G. Pollet, Journal of Power Sources, 2012. **208**: p. 96-119.
3. A. Rabis, P. Rodriguez, and T.J. Schmidt, Acs Catalysis, 2012. **2**(5): p. 864-890.
4. F. Takasaki, et al., Journal of the Electrochemical Society, 2011. **158**(10): p. B1270-B1275.
5. T. Tsukatsune, et al., Polymer Electrolyte Fuel Cells 10, Pts 1 and 2, 2013. **58**(1): p. 1251-1257.
6. K. Kanda, et al., ECS Electrochemistry Letters, 2014. **3**(4): p. F15-F18.
7. K. Grossmann, et al., Sensors and Actuators B-Chemical, 2011. **158**(1): p. 388-392.
8. L. Mädler, et al., Sensors and Actuators B-Chemical, 2006. **114**(1): p. 283-295.
9. L. Mädler, et al., Journal of Nanoparticle Research, 2006. **8**(6): p. 783-796.
10. A.T. Güntner, et al., ACS Sensors, 2016. **1**(5): p. 528-535.
11. Q. Fu, et al., Acs Applied Materials & Interfaces, 2015. **7**(50): p. 27782-27795.
12. P.I. Dahl, et al., MRS Proceedings, 2015. **1747**.
13. M.S. Thomassen, et al., ECS Transactions, 2011. **35**(34): p. 271-279.
14. D. Yang, et al., Chemistry of Materials, 2008. **20**(14): p. 4677-4681.
15. J. Zhang, et al., Transactions of Nonferrous Metals Society of China, 2014. **24**(1): p. 131-135.
16. M. Yin, et al., Applied Catalysis B-Environmental, 2014. **144**: p. 112-120.
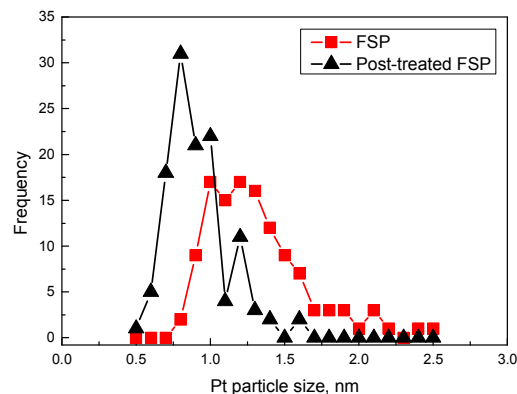17. W.Y Teoh, et al., Chemical Engineering Science, 2005. **60**(21): p. 5852-5861.